

# MeMo: Attentional Momentum for Real-time Audio-visual Speaker Extraction under Impaired Visual Conditions

Junjie Li\*, Wenxuan Wu\*, Shuai Wang†, Zexu Pan, Kong Aik Lee, Helen Meng, Haizhou Li

**Abstract**—Audio-visual Target Speaker Extraction (AV-TSE) aims to isolate a target speaker’s voice from multi-speaker environments by leveraging visual cues as guidance. However, the performance of AV-TSE systems heavily relies on the quality of these visual cues. In extreme scenarios where visual cues are missing or severely degraded, the system may fail to accurately extract the target speaker. In contrast, humans can maintain attention on a target speaker even in the absence of explicit auxiliary information. Motivated by such human cognitive ability, we propose a novel framework called MeMo, which incorporates two adaptive memory banks to store attention-related information. MeMo is specifically designed for real-time scenarios: once initial attention is established, the system maintains attentional momentum over time, even when visual cues become unavailable. We conduct comprehensive experiments to verify the effectiveness of MeMo. Experimental results demonstrate that our proposed framework achieves SI-SNR improvements of at least 2 dB over the corresponding baseline.

**Index Terms**—Memory Bank, Audio-visual Target Speaker Extraction, Attentional Momentum, Real-time, Visual Missing

## I. INTRODUCTION

Humans possess the remarkable ability to focus attention on a specific speaker while filtering out unwanted noise, a phenomenon known as ‘selective auditory attention’ [1], [2]. Beyond auditory information, human attention is inherently multi-modal, with visual inputs enhancing speech intelligibility [3], [4]. These multi-modal cues are processed interactively in the brain, complementing and enhancing one another to support perception and attention in complex environments.

Inspired by this, Audio-visual Target Speaker Extraction (AV-TSE) systems leverage multi-modal information, such as dynamic lip sequences, static face images, or body gestures [5]–[16], to emulate humans’ selective attention capabilities, thereby isolating the target speaker’s speech. AV-TSE plays a crucial role in enabling downstream tasks such as speech recognition [17], speaker diarization [18], and speaker verification [19]. By incorporating visual information, AV-TSE outperforms audio-only approaches, as visual cues are inherently robust to acoustic interference and provide complementary information to enhance target speech extraction.

Nevertheless, real-world scenarios often present challenges where visual cues of the target speaker may be unavailable or unreliable due to obstructions (e.g., mask-wearing), positional constraints (e.g., location outside the camera’s field of view), or degraded image quality. Under these conditions, the performance of AV-TSE systems deteriorates significantly [20]–[30].

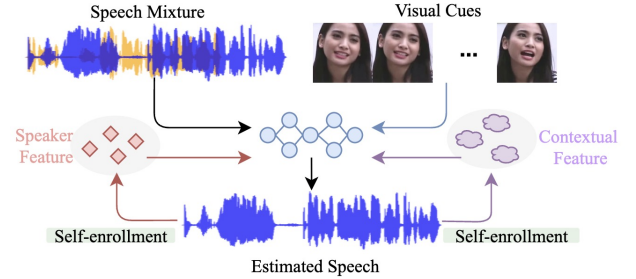


Fig. 1: Typical AV-TSE relies solely on visual cues, but performance drops when these cues are unreliable. In contrast, our proposed MeMo enhances reference information by incorporating speaker identity and contextual features through self-enrollment, ensuring more robust target speaker extraction.

Neuroscientific research [31]–[33] has shown that humans can enhance their selective auditory attention over time when concentrating on a specific sound source. This improvement is facilitated by the integration of multiple sensory and cognitive cues, including vocal characteristics, visual context, spatial localization, and contextual comprehension [32], [34], [35]. A fundamental neural mechanism supporting this process is working memory [36], [37], which plays a crucial role in maintaining and updating the current focus of attention.

Inspired by the human ability to sustain selective auditory attention, we propose a novel framework, MeMo<sup>1</sup>, which achieves *Attentional Momentum* through the use of *Adaptive Memory Banks*. Attentional momentum refers to the system’s capacity to maintain consistent focus on the target speaker over time, even when explicit reference information is unavailable. This ability closely mirrors the human phenomenon of ‘look once to hear,’ where a single glance at visual cue can anchor a sustained auditory focus, enabling enhanced speech extraction even in the absence of continuous visual inputs [38]. The memory banks serve as repositories for storing the model’s target attention, enabling continuity in speaker extraction. This functionality allows MeMo to emulate the human-like ability to effectively track a target speaker, even from limited visual information or after just a single observation.

MeMo is not tied to a specific model, instead it represents a generalizable concept that can be integrated into various model architectures. In this paper, we apply MeMo to the real-time single-channel target speaker extraction problem, where only voice characteristics and contextual information

\*: Equal contribution †: Corresponding author

<sup>1</sup>Code and demo: [https://mrjunjieli.github.io/demo\\_page/MeMo/index.html](https://mrjunjieli.github.io/demo_page/MeMo/index.html)

are available to compensate for missing visual cues, thereby reinforcing the TSE process. To achieve this, we design two types of memory banks: a speaker bank and a contextual bank. At the beginning of a conversation, these banks are empty, requiring visual cues to initialize the extraction process. Over time, speaker identity and contextual features are dynamically extracted from historically extracted speech which we refer to as self-enrollment speech, ensuring continuous adaptation and improved performance, as shown in Fig. 1.

The contributions of this paper are summarized as follows:

- We propose the concept of attentional momentum for AV-TSE, inspired by human cognitive mechanisms that maintain auditory focus despite visual impairments.
- We design MeMo, a generalizable framework with dual adaptive memory banks (speaker and contextual) that implements attentional momentum across various AV-TSE architectures.
- We validate MeMo’s effectiveness through comprehensive experiments on visually impaired VoxCeleb2 datasets, achieving consistent improvements across multiple evaluation metrics.
- We introduce an audio-visual speaker-switching evaluation dataset to assess system robustness when target speakers change dynamically during conversations.

## II. RELATED WORK

### A. Visual Impairments in AV-TSE

AV-TSE models typically rely on visual cues to extract target speech, but their performance deteriorates significantly when high-quality visual cues are absent or unreliable [8]. To address this challenge, Sadeghi and Alameda-Pineda [22], [23] propose bypassing the audio-visual variational auto-encoder (VAE) when visual cues are unreliable and instead using an audio-only VAE model. Wu et al. [24] and Pan et al. [21] incorporate an attention-based interaction mechanism, which dynamically utilizes adjacent available visual frames to extract target speech when visual cues are partially impaired. Rather than implicitly inpainting corrupted visual cues, ImagineNET [25] explicitly reconstructs them through audio-visual correspondence, employing a repeatedly interlaced structure. Additionally, the VS model [26] and the audio-visual SpeakerBeam [39], [40] utilize a speaker embedding to complement corrupted visual cues. Beyond using speaker embeddings as auxiliary information, Xu et al. [27] further incorporate spatial cues to handle scenarios where visual information is unavailable. Unlike models that directly integrate visual cues as inputs, Liu et al. [28], [29] propose learning audio-visual correlations using a consistency loss, where visual cues are used only during training. While the studies mentioned above primarily focus on offline scenarios, we aim to tackle the challenge of missing visual cues in real-time streaming environments. To address this, we introduce a novel approach that mimics the attentional momentum mechanism in the human brain, leveraging various types of information, such as audio, visual and contextual cues, as reference signals to maintain focus on the target speaker. Our previous work, MoMuSE [20], was an initial attempt to realize this concept, but it is a specific model which can not be generalized to any extraction models.

### B. Adaptive Memory Bank

Due to the limited receptive fields of traditional models, they struggle to effectively leverage long-term memory components. To overcome this limitation, memory networks have been proposed [41], [42], inspired by the storage mechanisms found in modern computers. These models are specifically designed to learn how to store, update, and retrieve new features within a memory component, enabling them to handle long-term dependencies and enhance performance.

Wu et al. [43] use a memory bank to store visual feature embeddings for all training samples, which eliminates the need to repeatedly compute representations. By maintaining a global view of instance features, the memory bank enables efficient scaling to large datasets. In multi-modal tasks, memory banks have been employed to store audio-visual mapping relations, facilitating the retrieval of clean speech information using only visual modalities during the inference stage. This method addresses the limitation of insufficient lip movement information in visual speech recognition [44]–[48], supports speech reconstruction from silent video [46], [49], and improves audio-visual speech recognition under noisy conditions [17]. Xu et al. [50] modeled attention and memory mechanisms for auditory selection using a pre-trained memory bank with fixed slots, similar to the approach in [44]. Bellur et al. [51] introduced a unified framework for speech and music source separation, utilizing the concept of temporal coherence to simulate selective auditory attention, gated by embeddings stored in memory.

Incorporating memory banks into these frameworks helps bridge the gap between limited temporal information and the ability to maintain long-term focus on relevant auditory and visual cues, aligning with the attentional momentum mechanism observed in human cognition.

### C. Self-enrollment Mechanism

In the self-enrollment mechanism, the model’s output is re-incorporated as new input, enabling the system to continuously refine and update its focus based on past predictions. Unlike methods that rely on irrelevant pre-enrolled speech, this approach has demonstrated greater effectiveness in TSE systems [26], [52]. Some studies suggest re-encoding the output from earlier layers as input for later ones [5], [53]. Other approaches operate in two stages, where the initial output serves as identity information, which is then used to guide the model’s second-stage processing [26], [54]. In online real-time scenarios, speech is processed incrementally, with each step utilizing the output from the previous step to continually adapt and refine the extraction process [55]–[62].

MeMo employs this self-enrollment strategy, extracting both speaker identity and contextual information from the self-enrolled speech. In online settings, this speech provides historical context and crucial speaker identity details, ensuring consistent speaker output.

## III. MEMO

### A. Problem Formulation

Audio-visual target speaker extraction [8], [9] seeks to isolate the target speech from a multi-speaker mixture by

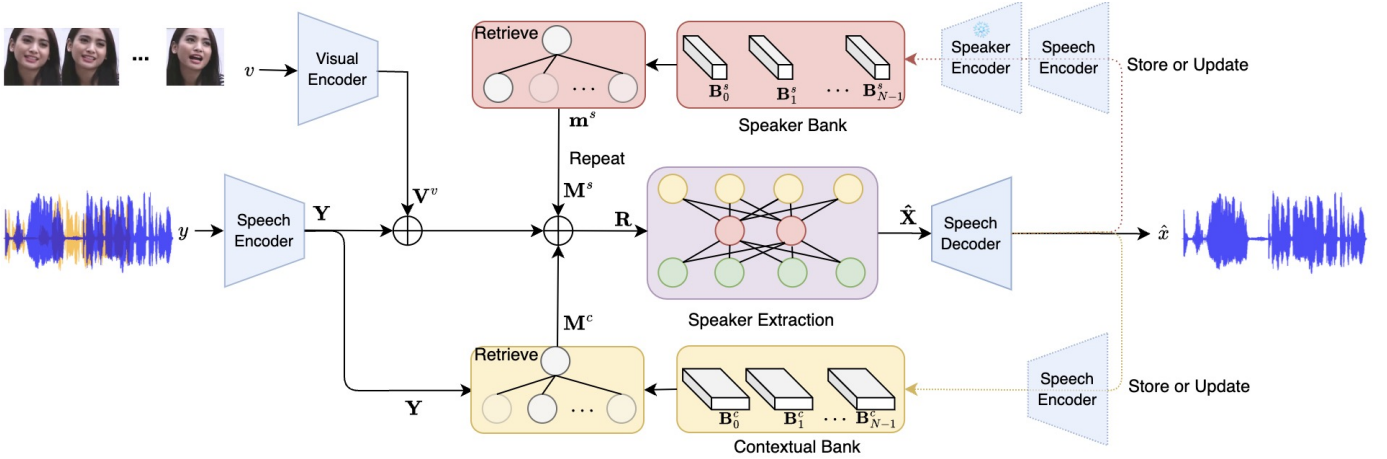


Fig. 2: Overview of MeMo framework. MeMo consists of two types of adaptive memory banks: speaker bank and contextual bank. The speaker bank contains  $N$  speaker embeddings, denoted as  $\mathbf{B}_n^s$ , while the contextual bank contains  $N$  speech embeddings, denoted as  $\mathbf{B}_n^c$ . The operator  $\oplus$  denotes concatenation. The parameters of three speech encoders are same. And the speaker encoder is pre-trained and frozen during training.

leveraging visual cues, such as the target speaker’s dynamic lip sequences in this paper. The problem could be formulated as follows:

$$\hat{x} = f_{\text{AV-TSE}}(y, v; \theta), \quad (1)$$

where  $y$  denotes mixture,  $\hat{x}$  represents the extracted speech,  $v$  denotes target visual cues,  $\theta$  is the parameter of AV-TSE model. The mixture  $y$  consists of multiple speech signals:

$$y[t] = x[t] + \sum_{i=1}^I s_i[t], \quad (2)$$

where  $x[t]$  and  $s_i[t]$  denote target speech and  $i$ -th interference speech signals, respectively.  $t$  indicates a discrete-time index.

For a general AV-TSE system, there are four basic modules: the speech encoder, visual encoder, speaker extractor, and speech decoder. Let  $y \in \mathbb{R}^{T \times 1}$  denote a time-domain speech mixture waveform, where  $T$  denotes the length of speech. The speech encoder transforms it into a latent speech embedding  $\mathbf{Y} \in \mathbb{R}^{L \times C}$ , where  $L$  and  $C$  represent the length and channel dimensions of the latent embeddings, respectively. Similarly, the visual encoder processes a visual sequence  $v \in \mathbb{R}^{\frac{T \cdot \text{sr}^v}{\text{sr}^a} \times H \times H}$  into a visual embedding  $\mathbf{V}^v \in \mathbb{R}^{L \times C}$ , where  $\text{sr}^v$  and  $\text{sr}^a$  denote the sample rate of visual sequence and audio sequence, respectively.  $H$  denotes the width and height of one visual frame. The speaker extractor estimates a mask to generate the estimated speech embedding  $\hat{\mathbf{X}} \in \mathbb{R}^{L \times C}$ , with visual cues as reference. The speech decoder then reconstructs the estimated speech waveform  $\hat{x} \in \mathbb{R}^{T \times 1}$ .

## B. System Overview

In this study, we aim to develop a robust AV-TSE system for real-world scenarios, where extraction operates as a streaming process and target visual cues may be unavailable.

Inspired by human attentional momentum, we propose MeMo, a novel framework that is not tied to a specific model but can be integrated into various separation backbones. MeMo introduces two types of adaptive memory banks: a speaker

bank and a contextual bank, as illustrated in Fig. 2. Unlike conventional AV-TSE systems that rely solely on visual cues as reference, MeMo retrieves speaker identity and contextual information from memory banks as supplementary references. This mechanism effectively addresses challenges posed by impaired visual cues in real-world conditions.

Notably, both memory banks are adaptive rather than pre-trained and frozen. At the start of the online processing, these banks are empty. Once the estimated speech is extracted from the first processing window, it is self-enrolled as a speaker embedding and a contextual speech embedding, which are then stored in their respective banks. As the memory banks fill up, an updating mechanism dynamically replaces older embeddings with new ones, ensuring continuous adaptation.

As introduced above, attentional momentum is achieved by consistently extracting attention information from the historically estimated speech, ensuring that attention remains focused on the same speaker over time. Additionally, current visual cues are also utilized. The balance between historical and current information makes the model well-suited for real-world conditions, even in target speaker switching scenarios, where the target speaker may change during a conversation. We will discuss this in Section III-D.

## C. Adaptive Memory Bank

As mentioned in the system overview, we employ two types of adaptive memory banks to store the tracking signals for the target speaker: speaker identity cues and historical contextual information of conversation. In this section, we will introduce how to retrieve the most relevant speaker cues and contextual cues from these memory banks.

1) *Speaker Bank*: Suppose the speaker bank has  $N$  slots, each slot contains a speaker embedding. The speaker bank could be represented as:  $\mathbf{B}^s = \{\mathbf{B}_0^s, \mathbf{B}_1^s, \dots, \mathbf{B}_{N-1}^s\}$ , where  $\mathbf{B}_n^s \in \mathbb{R}^{1 \times C}$  denotes the  $n$ -th slot and  $\mathbf{B}^s \in \mathbb{R}^{N \times C}$  denotes the whole speaker bank, as shown in Fig. 3.

Considering the intra-speaker variability of different speaker slots [8], we want to effectively capture the most relevant



Fig. 3: Illustration of retrieval operation from speaker bank.

speaker cues correlated with the target speaker in the current mixture frames, we apply a self-attention [63] mechanism over the entire speaker bank  $\mathbf{B}^s$ . Specifically, we compute the self-attention using the speaker bank as the query, key, and value:

$$\mathbf{Q}, \mathbf{K}, \mathbf{V} \in \mathbb{R}^{N \times C} = \text{Linear}(\mathbf{B}^s), \quad (3)$$

where ‘Linear’ transformation projects the input embeddings into a new representation space. Then, a softmax operation is applied along the first dimension, and the attention score matrix among different speaker slots is computed as follows:

$$\mathbf{A} \in \mathbb{R}^{N \times N} = \text{softmax} \left( \frac{\mathbf{Q}\mathbf{K}^\top}{\sqrt{C}}, \text{dim}=1 \right). \quad (4)$$

Then we compute the average score on dimension zero to get the final attention weight for each speaker embedding:

$$\bar{\mathbf{A}} \in \mathbb{R}^{1 \times N} = \text{AvgPooling}(\mathbf{A}, \text{dim}=0). \quad (5)$$

Then the most relevant speaker cue  $\mathbf{m}^s$  is obtained:

$$\mathbf{m}^s \in \mathbb{R}^{1 \times C} = \bar{\mathbf{A}}\mathbf{V}. \quad (6)$$

To align with mixture embedding  $\mathbf{Y}$ ,  $\mathbf{m}^s$  is repeated along length dimension to get  $\mathbf{M}^s \in \mathbb{R}^{L \times C}$ .

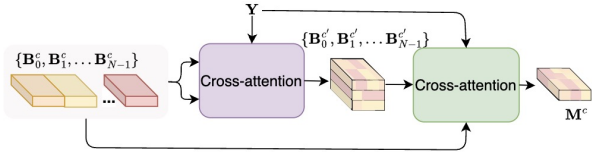


Fig. 4: Illustration of retrieval operation from contextual bank.

2) *Contextual Bank*: Similar to the speaker bank, the contextual bank contains  $N$  slots:  $\mathbf{B}^c = \{\mathbf{B}_0^c, \mathbf{B}_1^c, \dots, \mathbf{B}_{N-1}^c\}$ , where  $\mathbf{B}_n^c \in \mathbb{R}^{L \times C}$  and  $\mathbf{B}^c \in \mathbb{R}^{N \times L \times C}$  denote the  $n$ -th slot and whole contextual bank, respectively. In this case, we employ two cross-attention layers to retrieve the most relevant contextual information, as shown in Fig. 4.

The first cross-attention layer is employed for  $N$  times to capture the most relevant content from each contextual slot  $\mathbf{B}_n^c$  based on the mixture embedding  $\mathbf{Y}$ :

$$\mathbf{K} \in \mathbb{R}^{L \times C} = \text{Linear}(\mathbf{Y}), \quad (7)$$

$$\mathbf{Q}, \mathbf{V} \in \mathbb{R}^{L \times C} = \text{Linear}(\mathbf{B}_n^c). \quad (8)$$

Then filtered contextual speech embedding is obtained:

$$\mathbf{B}_n^{c'} \in \mathbb{R}^{L \times C} = \text{softmax} \left( \frac{\mathbf{Q}\mathbf{K}^\top}{\sqrt{C}}, \text{dim}=1 \right) \mathbf{V}. \quad (9)$$

The second attention is also a cross-attention, aiming to obtain a global contextual information from different slots. In this case, key, query and value are computed as follows:

$$\mathbf{K} \in \mathbb{R}^{L \times C} = \text{Linear}(\mathbf{Y}), \quad (10)$$

$$\mathbf{Q} \in \mathbb{R}^{L \times N \times C} = \text{Linear}(\mathbf{B}^{c'}), \quad (11)$$

$$\mathbf{V} \in \mathbb{R}^{L \times N \times C} = \text{Linear}(\mathbf{B}^c). \quad (12)$$

Then the softmax operation is used to compute the weight for each slot <sup>2</sup>:

$$\mathbf{A} \in \mathbb{R}^{L \times N} = \text{softmax} \left( \frac{\mathbf{Q}\mathbf{K}}{\sqrt{C}}, \text{dim}=1 \right). \quad (13)$$

Here, the attention score  $\mathbf{A}$  denotes the weight for each contextual slot. Then the most relevant contextual speech embedding is obtained by weighting different slots:

$$\mathbf{M}^c \in \mathbb{R}^{L \times C} = \mathbf{A}\mathbf{V}. \quad (14)$$

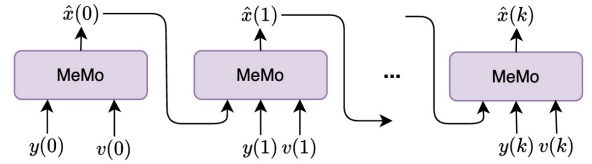


Fig. 5: The basic idea of attentional momentum.  $y(k)$ ,  $v(k)$  and  $\hat{x}(k)$  denote the speech mixture, visual cues and estimated speech at the  $k$ -th online window step.

#### D. Attentional Momentum

The attentional momentum mechanism refers to the human ability to maintain focus on a specific speaker over time during a conversation. Our goal is to replicate this ability in AV-TSE systems. We first implemented this concept in MoMuSE [20], achieving convincing results.

In online scenarios, as shown in previous work [20], [59], [60], input speech is processed using a sliding window. This window shifts gradually over time, with each step incorporating new data for speaker extraction. Fig. 5 shows the core concept of attentional momentum. At the start of online processing, MeMo initially relies on visual cues for speaker extraction. As the process continues, the model incorporates previously estimated speech as additional reference, helping to maintain a consistent focus on the target speaker.

Based on the adaptive memory banks, the attentional momentum mechanism could be summarized into three components: storing, retrieval, and updating:

- **Storing**: Suppose the volume of each memory bank is  $N$ . Then during the  $k$ -th ( $N - 1 \geq k \geq 0$ ) online processing window step, these memory banks are not full. The estimated speech  $\hat{x}(k)$  at  $k$ -th window step, is processed by the speech encoder and speaker encoder to generate a contextual speech embedding  $\mathbf{B}_k^c$  and speaker embedding  $\mathbf{B}_k^s$ , as illustrated by the dotted lines in Fig. 2. These embeddings are then stored in their respective

<sup>2</sup>We omit some dimension transpose operations for simplicity.

memory banks. We utilize a pre-trained ECAPA-TDNN [64] from WeSpeaker [65] as the speaker encoder<sup>3</sup>. The structure and parameters of the speech encoder in Fig. 2 are totally the same. It is important to note that  $\hat{x}(0)$  is predicted solely using visual cues  $v(0)$ , cause the memory banks are empty at that time. After the 0-th window step, the extraction processing is guided by multiple cues, including visual cues, speaker cues and contextual cues retrieved from the adaptive memory banks.

- **Retrieval:** As introduced in Section III-C, MeMo employs an attention-based mechanism to retrieve the most relevant information from all slots in the memory banks. Instead of selecting a single slot, MeMo leverages attention weights to fuse information from all slots, enhancing the model’s ability to maintain long-term consistency. At the  $k$ -th window step, where  $k > 0$ , memory banks are not empty. MeMo generates momentum speaker features  $\mathbf{M}^s(k)$  and momentum contextual features  $\mathbf{M}^c(k)$  to keep model’s attention at  $k$ -th window step in line with previous steps. Hence, the final concated features are shown below:

$$\mathbf{R}(k) = \mathbf{Y}(k) \oplus \mathbf{V}(k) \oplus \mathbf{M}^s(k) \oplus \mathbf{M}^c(k), \quad (15)$$

where  $\oplus$  denotes concatenation.  $\mathbf{Y}$ ,  $\mathbf{V}$ ,  $\mathbf{M}^s$  and  $\mathbf{M}^c$  denotes mixture feature, visual feature, speaker feature and contextual features, respectively.

- **Updating:** Suppose the memory bank can store up to  $N$  feature slots. At the  $k$ -th window step, where  $k \geq N$ , these banks are full. We design two methods to pop out the old embedding and insert the new one.
  - FIFO: Like a queue in a computer system, once the memory bank reaches its maximum capacity, the oldest feature is discarded following a first-in-first-out policy. This ensures that the memory bank always contains the most recent features for extraction.
  - ABS: To further enhance adaptability, we propose an alternative updating method called attention-based selection (ABS). In this method, instead of always discarding the oldest feature, the feature with the lowest attention score (computed as shown in Equation 13 and Equation 5) is removed from the bank.

### E. Training and Inference Strategy

MeMo is designed for online processing scenarios, making it highly applicable to real-world applications. The attentional momentum mechanism enables MeMo to maintain attention on the same speaker over time. To achieve this, autoregressive (AR) training strategy is a straightforward approach. However, the computational cost is high, and errors can accumulate easily. To address this, we adopt a pseudo-autoregressive (PAR) training approach, similar to PARIS [61].

1) *PAR Training Strategy:* As shown in Algorithm 1, the proposed PAR strategy contains two stages. The first stage aims to get a self-enrolled estimated speech  $\hat{x}^1$ . The second stage utilizes  $\hat{x}^1$  as new reference to get the final output  $\hat{x}^2$ .

---

**Algorithm 1** The pseudo python code for PAR.

---

**Inputs:** speech mixture  $y$ , visual inputs  $v$ , pre-enrolled speech  $p$

**# Stage 1**

$$\hat{x}^1 = \begin{cases} f_{\text{AV-TSE}}(y, v, p; \theta), & \text{for VP}_{\text{Init}} \text{ only,} \\ f_{\text{AV-TSE}}(y, v; \theta), & \text{otherwise.} \end{cases} \quad (16)$$

**# Stage 2**

$$\alpha = \begin{cases} \frac{ep}{ep_{\text{cr}}}, & \text{if } ep \leq ep_{\text{cr}}, \\ 1, & \text{otherwise.} \end{cases}$$

$$\hat{x}_{\text{cr}}^1 = \alpha \cdot \hat{x}^1 + (1 - \alpha) \cdot \frac{\|\hat{x}^1\|^2}{\|x\|^2} \cdot x \text{ \# Curriculum learning}$$

$m = []$  \# memory bank

for  $i = 1$  to  $N$ : \# The number of slots in memory bank

$$\hat{x}_{\text{cut}}^1 = \hat{x}_{\text{cr}[0:T-i*T_{\text{sh}}]}^1$$

$$\hat{x}_{\text{pad}}^1 = \text{LeftZeroPadding}(\hat{x}_{\text{cut}}^1)$$

$$m.\text{append}(\hat{x}_{\text{pad}}^1)$$

$$m_{\text{shuf}} = \text{shuffle}(m)$$

$$\hat{x}^2 = f_{\text{AV-TSE}}(y, v, m_{\text{shuf}}; \theta)$$

**# Total Loss**

$$\mathcal{L} = \beta \mathcal{L}_{\text{SI-SNR}}(\hat{x}^1, x) + (1 - \beta) \mathcal{L}_{\text{SI-SNR}}(\hat{x}^2, x).$$


---

**Stage 1:** The model performs extraction using only the visual cue  $v$  as the reference. While for speaker bank training, we find that utilizing an additional pre-enrolled speech  $p$  which is easy to obtain in real-world scenarios, contributes to improve the quality of  $\hat{x}^1$ . We refer to this setting as  $\text{VP}_{\text{Init}}$ . The alternative setting, where only the visual cue  $v$  is used without the pre-enrolled speech, is referred to as  $\text{V}_{\text{Init}}$ .

**Stage 2:** We utilize the self-enrolled estimated speech  $\hat{x}^1$  as reference together with visual cues. However, at early training epochs, the quality of  $\hat{x}^1$  is often poor because the model has not yet converged, which can destabilize training [55]–[58], [61]. To mitigate this issue, we adopt a curriculum learning strategy [66]–[68], gradually transitioning from the ground truth target speech  $x$  to the self-enrolled speech  $\hat{x}^1$ . Specifically, we define a new curriculum-guided speech  $\hat{x}_{\text{cr}}^1$ , where the curriculum weight  $\alpha$  increases linearly from 0 to 1 over the first  $ep_{\text{cr}}$  epochs. After that,  $\hat{x}_{\text{cr}}^1$  fully degenerates into  $\hat{x}^1$ , enabling the model to rely solely on its own self-enrollment speech. Cause we use signal-to-noise ratio (SI-SNR) as training loss, the energy of  $\hat{x}^1$  is not stable. Hence  $\frac{\|\hat{x}^1\|^2}{\|x\|^2}$  is used to reduce the energy gap. To teach the model how to select the most relevant slot from memory bank, we create a memory  $m$  to mimic this processing.  $\hat{x}_{\text{cr}}^1$  is segmented into  $N$  overlapping speech, with each shifts  $T_{\text{sh}}$  samples. Each segment is left-padded to the original length  $T$  to maintain shape consistency. To avoid overfitting to temporal continuity, the memory bank is randomly shuffled before being used as the reference in training.

The training loss will be computed both on  $\hat{x}^1$  and  $\hat{x}^2$ , and could be expressed as:

$$\mathcal{L} = \beta \mathcal{L}_{\text{SI-SNR}}(\hat{x}^1, x) + (1 - \beta) \mathcal{L}_{\text{SI-SNR}}(\hat{x}^2, x), \quad (17)$$

<sup>3</sup>[https://wenet.org.cn/downloads?models=wespeaker&version=voxceleb\\_ECAPA512.zip](https://wenet.org.cn/downloads?models=wespeaker&version=voxceleb_ECAPA512.zip)

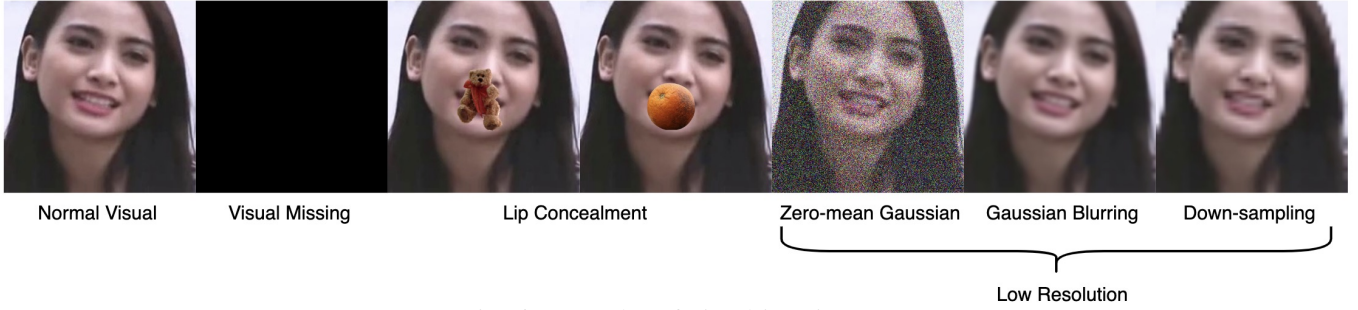


Fig. 6: Examples of visual impairments.

where  $\mathcal{L}_{\text{SI-SNR}}$  is defined as :

$$\mathcal{L}_{\text{SI-SNR}}(\hat{x}, x) = -10 \log_{10} \frac{\|\frac{\langle \hat{x}, x \rangle x}{\|\hat{x}\|^2}\|^2}{\|\hat{x} - \frac{\langle \hat{x}, x \rangle x}{\|\hat{x}\|^2}\|^2}. \quad (18)$$

TABLE I: Online processing parameters descriptions.

Parameter	Description
$T_{\text{win}}$	Duration of sliding window (in samples). $T_{\text{win}}$ is the receptive field of models.
$T_{\text{sh}}$	Duration of window shifting length (in samples). The sliding window moves $T_{\text{sh}}$ every time.
$T_{\text{init}}$	Duration of cold start time (in samples). The incoming data accumulates to $T_{\text{init}}$ before starting.

2) *Online Inference Strategy*: In online real-time processing [20], [59], [60], the model begins processing once the accumulated input reaches a predefined initialization length, denoted as  $T_{\text{init}}$ , which corresponds to the 0-th window step. The first stage in Algorithm 1 simulates this initialization step. After that, the model processes speech using a sliding window of length  $T_{\text{win}}$ , with the window shifting forward by  $T_{\text{sh}}$  at each step. All parameters are summarized in Table I.

In most cases, the model uses only visual cues as reference during the initialization step. However, in the  $\text{VP}_{\text{init}}$  setting of the speaker bank, both the visual cue and the pre-enrolled speech are used as reference for initialization.

Cause we use  $\mathcal{L}_{\text{SI-SNR}}$  as loss function, then energy of estimated speech for each window step is different. To ensure the perception consistency, we utilize the energy normalization strategy applied in [59] to smooth the overall output. We normalize  $\hat{x}(k)$  based on the energy between current window step and all previous window steps:

$$\hat{x}(k) = \begin{cases} \gamma \cdot \frac{\hat{x}(k)}{\|\hat{x}(k)\|^2} & \text{k=0} \\ \hat{x}(k) \cdot \frac{\|\hat{x}[0:k-1]\|^2}{\|\hat{x}(k)\|^2} & \text{otherwise,} \end{cases} \quad (19)$$

where  $\gamma$  is a normalization weight aims to control the energy of the speech.

## IV. EXPERIMENTAL SETUP

### A. Dataset

1) *Visual Impairments*: We simulate three types of impaired scenarios: visual missing, lip concealment, and low resolution, as shown in Fig. 6.

- **Visual missing**: the speaker’s face is undetected, hence the whole visual frame is set to zero values.
- **Lip concealment**: Target speaker’s lip is occluded by a certain obstacle, such as hands or microphones. We utilize the Naturalistic Occlusion Generation (NatOcc) dataset [69] to simulate this, similar to [70]<sup>4</sup>. The NatOcc patches consist of various objects, such as fruits, desserts, cups, and so on. For evaluation fairness, we reserve one specific object for the test set, and other objects are randomly selected on-the-fly during training.
- **Low resolution**: Visual frames are not recorded clearly and appear blurry. We utilize three methods to simulate this: zero-mean Gaussian noise<sup>5</sup>, Gaussian blurring<sup>6</sup> and image down-sampling. For the training and validation sets, zero-mean Gaussian noise and Gaussian blurring are selected with equal probability to capture a range of blurriness levels. For the test set, only image down-sampling is applied.

2) *VoxCeleb-2mix*: We construct a two-speaker mixture dataset from the VoxCeleb2 dataset [71], where each mixture consists of a target speaker and an interfering speaker. To ensure diversity of speaker and utterances, we select a wide range subset from VoxCeleb2, including 48,000 utterances from 800 speakers for training set and validation set simulation and 36,237 utterances from 118 speakers for test set simulation, following [5], [72], [73]. Specifically, we simulate 20,000 utterances for the training set, 5,000 for the validation set, and 3,000 for the test set. Each target utterance is mixed with an interfering utterance at a random signal-to-noise ratio (SNR) between -10 dB and 10 dB, temporally aligned with the short utterance. The audio sampling rate  $\text{sr}^a$  is 16,000 Hz, and the video frame rate  $\text{sr}^v$  is 25 FPS. None of the speakers in the test set were encountered during training and validation. Utterances are limited to 4-6 seconds during training and real duration during inference. For each utterance, only one type of impairment has been selected. The impairment ratio is randomly chosen from [0%, 80%) for the training and validation sets, and from [0%, 100%) for the test set.

3) *VoxCeleb-2mix-switch*: We build a test set to simulate two target speakers switching in a cocktail party, as shown in Fig. 7. To make sure there are always two speakers speaking,

<sup>4</sup><https://github.com/joannahong/AV-ReIScore>

<sup>5</sup>[https://scikit-image.org/docs/0.23.x/api/skimimage.util.html#skimimage.util.random\\_noise](https://scikit-image.org/docs/0.23.x/api/skimimage.util.html#skimimage.util.random_noise)

<sup>6</sup><https://pytorch.org/vision/main/generated/torchvision.transforms.GaussianBlur.html>



Fig. 7: An example of target speaker switching during a conversation is illustrated in this figure. Attention shifts from one target speaker to another at a certain point, while interfering speech or background noise persists.

the interfering speaker simultaneously speaks for at least 10 seconds. The switch point occurs randomly between 4 and 6 seconds. To achieve this, we select utterances within least 10 seconds from the VoxCeleb2 test set and simulate 3000 mixtures. The visual cue impaired setting is the same as VoxCeleb-2mix, except we also ensure visual cues are clean for 1 second after the switch point, for smooth cool start purposes. Other settings are the same with VoxCeleb-2mix. The interfering utterance is mixed at a random SNR between -10 dB and 10 dB.

### B. Metrics

We select the SI-SNR [74], SDR<sup>7</sup> [74], perceptual evaluation of speech quality (PESQ)<sup>8</sup> [75] and the short-term objective intelligibility (STOI)<sup>9</sup> [76] as metrics to evaluate signal similarity and speech quality. Higher values denote better performance.

In online evaluation, we use a real-time factor (RTF) to express the model’s computational complexity, the lower the better. It is calculated using a NVIDIA Tesla V100 GPU, and is given by the following formula:

$$\text{RTF} = \frac{\text{Processing Time}}{\text{Speech Length}}. \quad (20)$$

### C. Implementation Details

1) *Training*: The initial learning rate was set to 1e-3 using the Adam optimizer. The learning rate was halved if the best validation loss (BVL) did not improve within six consecutive epochs, and the training stopped if the BVL did not improve within ten consecutive epochs. The maximum number of training epochs was set to 100. The  $\text{epoch}_{\text{curr}}$  was set to 50 for curriculum learning. The number of slots  $N$  in memory banks was randomly chosen from [1, 5]. During training, the window shift  $T_{\text{sh}}$  was set within  $[0, sr^a]$ . The loss weight  $\beta$  was set to 0.2.

2) *Inference*: The online parameters  $T_{\text{win}}$ ,  $T_{\text{sh}}$ , and  $T_{\text{init}}$  were set to  $2sr^a$ ,  $0.2sr^a$ , and  $2sr^a$ , respectively. In the 0-th window step, clean visual frames without impairments were used to ensure high-quality self-enrolled speech. The number of slots  $N$  in each memory bank was set to 1 by default, and the duration of self-enrolled speech was also fixed at 2 seconds by default. Additionally, clean visual cues were used

for initialization at the 0-th step. The normalization weight  $\gamma$  was set to 0.7.

3) *Dataset*: The visual inputs were cut from the middle part of all face frames and transformed into grayscale with the size of  $112 \times 112$ . We applied visual impairments directly on video frames. For lip concealment case, the obstacle object was randomly positioned around the center of each frame with offsets of [13, 17]. For zero-mean gaussian, the noise variance was randomly selected from [0.02, 0.2]. For gaussian blurring, a 2D Gaussian filter with a kernel size of (13, 13) and standard deviations of (4, 8) was applied. For down-sampling, the resolution of video frames was reduced by a factor of 10.

TABLE II: Four types of evaluation settings in offline mode and online mode. We take the  $k$ -th window step as an example in online mode. Settings in gray represent the use of static reference inputs (i.e., pre-enrolled or ground-truth target speech) for comparison purposes. The underlined settings are the primary and novel settings proposed in this paper.

Evaluation Settings	Evaluation mode	Formulation
Visual Only	Offline Online	$\hat{x} = f_{\text{AV-TSE}}(y, v; \theta)$ $\hat{x}(k) = f_{\text{AV-TSE}}(y(k), v(k); \theta)$
<u>Visual+SelfEnro</u>	Offline <u>Online</u>	$\hat{x} = f_{\text{AV-TSE}}(y, v, f_{\text{AV-TSE}}(y, v; \theta); \theta)$ $\hat{x}(k) = f_{\text{AV-TSE}}(y(k), v(k), \hat{x}(k-1); \theta)$
Visual+PreEnro	Online Online	$\hat{x} = f_{\text{AV-TSE}}(y, v, p; \theta)$ $\hat{x}(k) = f_{\text{AV-TSE}}(y(k), v(k), p; \theta)$
Visual+TgtEnro	Offline Online	$\hat{x} = f_{\text{AV-TSE}}(y, v, x; \theta)$ $\hat{x}(k) = f_{\text{AV-TSE}}(y(k), v(k), x(k); \theta)$

## V. RESULTS AND ANALYSIS

In this section, we evaluate MeMo’s effectiveness across various scenarios and settings, focusing primarily on **online mode with impaired visuals**. To assess the impact of impaired visuals, we consider two scenarios:

- Clean Visual: The visual cues remain intact.
- Impaired Visual: Some visual frames are partially corrupted, as described in Section IV-A1.

For each visual scenario, we evaluate the models under four different settings, as shown in Table II. These evaluation settings are designed to compare the effectiveness of different types of reference information. Typical AV-TSE systems operate under the ‘Visual Only’ setting, where only visual cues are used. In contrast, our proposed model, MeMo, can leverage dynamic reference, self-enrolled speech from the previous window step under the ‘Visual+SelfEnro’ setting, which is the primary and novel setting introduced in this work. The ‘Visual+PreEnro’ and ‘Visual+TgtEnro’ settings are similar to ‘Visual+SelfEnro’, but they only use static reference, pre-enrolled speech and ground-truth target speech, respectively. Hence, memory banks are not applicable under these two settings, since the reference speech does not evolve over time. These settings are included as comparison to help evaluate the relative effectiveness of self-enrolled cues.

Unless specified otherwise, the results in this section are presented for **online mode with impaired visuals** under the ‘Visual+SelfEnro’ setting by default.”

<sup>7</sup><https://pyip.org/project/fast-bss-eval/>

<sup>8</sup><https://pyip.org/project/pesq/>

<sup>9</sup><https://pyip.org/project/pystoi/>

TABLE III: Comparison between different speaker banks in offline and online evaluation mode in terms of SI-SNR.  $V_{\text{Init}}$  and  $VP_{\text{Init}}$  are different speaker banks, as defined in Equation 16. N/A indicates that the item is not applicable in the given setting. Number of slots  $N$  in online mode is set to 1 by default during the inference stage.

Sys. #	Model	Speaker Bank		Evaluation Mode	SI-SNR (dB) $\uparrow$							
		$V_{\text{Init}}$	$VP_{\text{Init}}$		Clean Visual				Impaired Visual			
					Visual Only	<u>Visual+SelfEnro</u>	Visual+PreEnro	Visual+TgtEnro	Visual Only	<u>Visual+SelfEnro</u>	Visual+PreEnro	Visual+TgtEnro
	Mixture				0							
1	TDSE [77]			Offline	11.16		N/A		10.32	N/A		
2	MeMo (TDSE)	✓			11.23	11.31	11.31	11.40	10.25	10.35	10.52	10.69
3			✓		N/A	<b>11.46</b>	11.33	11.61	N/A	<b>10.84</b>	10.83	11.27
1	TDSE [77]			Online	9.55		N/A		8.13	N/A		
2	MeMo (TDSE)	✓			9.65	9.87	9.91	10.07	8.16	8.64	8.60	8.76
3			✓		N/A	<b>10.12</b>	10.05	10.48	N/A	<b>9.43</b>	9.24	9.85

TABLE IV: The impact of varying the number of memory slots in the online mode under the ‘Visual+SelfEnro’ setting for the impaired visual scenario. The length of self-enrolled speech refers to the audio duration used for self-enrollment, before being embedded into speaker embeddings. All results are reported in terms of SI-SNR (dB).

Sys. #	Length of Self-enrolled Speech (seconds)	Number of Slots $N$			
		1	2	4	
				FIFO	ABS
2	2s	8.64	8.66	8.66	<b>8.69</b>
	1s	8.62	8.64	8.64	8.67
	0.5s	8.60	8.60	8.62	8.67
3	2s	9.43	9.43	9.44	<b>9.48</b>
	1s	9.26	9.31	9.31	9.48
	0.5s	8.81	8.99	9.15	9.30

### A. Speaker Bank

Based on the differences in training methods, there are two types of speaker banks, as shown in Equation 16.  $V_{\text{Init}}$  represents the case where only visual cues are used for initialization, while  $VP_{\text{Init}}$  incorporates both visual cues and pre-enrolled speech to generate the self-enrolled speech during the initialization step. Table III presents the overall results of applying the speaker bank. We use TDSE, which is a time-domain model based on Conv-TasNet [78], as baseline model. In this table, MeMo adopts the same backbone structure like TDSE, but incorporates an additional speaker banks.

1) *Evaluation in Offline Mode:* Firstly, we evaluate the models in offline mode, where the entire utterance of speech is provided as input in inference. Several key observations can be drawn from the results:

- The performance gap between clean and impaired visual conditions is obvious. This supports our motivation that the quality of visual cues significantly affects extraction performance.
- Both types of speaker bank under ‘Visual+SelfEnro’ provide light but consistent performance improvements than Systems 1 especially with impaired visual cues. Between them,  $VP_{\text{Init}}$  performs better than  $V_{\text{Init}}$ , highlighting

the benefit of incorporating pre-enrolled speech during initialization.

- Among the four evaluation settings, ‘Visual+TgtEnro’ serves as an idealized upper bound. The ‘Visual+SelfEnro’ setting yields results similar to ‘Visual+PreEnro’ and outperforms the ‘Visual Only’ setting which performs the worst. This indicates that MeMo effectively leverages speaker information from self-enrolled speech.

2) *Evaluation in Online Mode:* Similarly, we compare different systems in online mode, which is our target evaluation mode in this paper.

- Compared to offline mode, system performance in online mode is generally lower. This is reasonable since the receptive field in online models is shorter, limiting the available information for extraction.
- The performance gap between the baseline (‘Visual Only’) and MeMo (‘Visual+SelfEnro’) is evident, particularly when using the  $VP_{\text{Init}}$  speaker bank under impaired visual scenarios, demonstrating the superior effectiveness of attentional momentum. These results suggest that our method is well-suited for online impaired scenarios.

3) *Impact of the Number of Slots:* In this section, we investigate how the number of slots affects model performance. As shown in Table IV, increasing the number of slots leads to performance gains, particularly for System 3. Notably, when the duration of self-enrolled speech is short, the model benefits more from having additional slots in the speaker bank. This suggests that the model can retrieve complementary speaker identity information across different slots. However, when sufficient speaker information is already available, adding more slots yields no significant improvement. Regarding different popping strategies, the attention-based selection (ABS) method provides a performance boost, though the improvement is relatively modest.

### B. Contextual Bank

Although the speaker bank contributes to performance improvement, the gains are relatively limited. This observation motivates us to explore the effectiveness of the contextual bank, which is designed to capture temporal and contextual



TABLE V: Performance of contextual bank under different evaluation settings. Here we only present one speaker bank,  $VP_{\text{Init}}$ . Number of slots  $N$  in online mode is set to 1 by default.

Sys. #	Model	Contextual Bank	Speaker Bank	Evaluation Mode	SI-SNR (dB) $\uparrow$								
					Clean Visual				Impaired Visual				
					Visual Only	Visual+SelfEnro	Visual+PreEnro	Visual+TgtEnro	Visual Only	Visual+SelfEnro	Visual+PreEnro	Visual+TgtEnro	
	Mixture				0								
1	TDSE [77]				11.16		N/A			10.32		N/A	
3	MeMo (TDSE)		✓	Offline	N/A	11.46	11.33	11.61	N/A	<b>10.84</b>	10.83	11.27	
4		✓			11.51	<b>11.63</b>	11.01	12.37	10.59	10.70	9.54	12.37	
5		✓	✓		N/A	11.35	11.25	11.65	N/A	10.73	10.60	11.53	
1	TDSE [77]				9.55		N/A			8.13		N/A	
3	MeMo (TDSE)		✓	Online	N/A	10.12	10.05	10.48	N/A	9.43	9.24	9.85	
4		✓			10.24	<b>10.50</b>	9.27	10.94	8.82	<b>10.34</b>	7.71	10.93	
5		✓	✓		N/A	10.33	10.64	10.01	N/A	10.04	9.05	10.41	

information. In this section, we present a detailed comparison between the speaker bank ( $VP_{\text{Init}}$ ) and the contextual bank, as shown in Table V. We summarize several key observations:

- While the ‘Visual+SelfEnro’ performance of contextual bank and speaker bank is similar in the offline mode, the contextual bank demonstrates obviously better effectiveness in the online mode.
- The contextual bank yields substantial performance gains over the baseline, particularly under impaired visual conditions in the online mode, which is our primary target scenario, with improvements exceeding 2 dB in SI-SNR.
- The ‘Visual+SelfEnro’ setting presents a significant improvement over ‘Visual+PreEnro’ and achieves results in online mode comparable to our upper-bound ‘Visual+TgtEnro’. This indicates that leveraging online contextual information plays a critical role in enhancing model performance, and our proposed method effectively utilizes nearly full contextual information.
- Combining the speaker bank with the contextual bank does not lead to complementary improvements. On the contrary, it degrades performance, resulting in worse outcomes than using the contextual bank alone, possibly due to redundancy or conflicting reference information.

TABLE VI: The impact of varying the number of memory slots in the online mode under the ‘Visual+SelfEnro’ setting for the impaired visual scenario. All results are reported in SI-SNR (dB).

Sys. #	Length of Self-enrolled Speech (seconds)	Number of Slots $N$			
		1	2	4	
				FIFO	ABS
4	2s	<b>10.34</b>	10.10	9.33	9.11
5	2s	<b>10.04</b>	9.83	9.62	9.54

Similarly, we analyze the impact of the number of slots in the contextual bank, as shown in Table VI. As the number of slots increases, performance gradually degrades. This aligns with our intuition: in the case of the contextual bank, the latest

contextual information is typically more relevant for current speaker extraction, and adding excessive historical information may introduce noise or conflicts. Regarding different popping strategies, the attention-based selection (ABS) method does not improve the performance of the contextual bank. This may be because contextual speech embeddings are relatively low-level representations, making it difficult for the attention mechanism to assign correct scores to different slots.

TABLE VII: Comparison results across different types of impaired visual cues under the online mode. The number of slots  $N$  for each system is set to 1 by default in this table. Results are reported in SI-SNR (dB).

Sys. #	Impaired			Clean	
	Visual Missing	Lip Concealment	Low Resolution	Avg.	Avg.
1	6.35	9.05	8.98	8.13	9.55
2	7.28	9.59	9.03	8.64	9.65
3	8.57	9.96	9.75	9.43	10.12
4	<b>10.18</b>	10.31	<b>10.52</b>	<b>10.34</b>	<b>10.50</b>
5	9.61	<b>10.46</b>	10.05	10.04	10.33

### C. Impact of the Impairment Types

As shown in Table VII, we report performance across three different types of impairments. For System 1, we evaluate its performance under the ‘Visual Only’ setting, while for other systems, we report their performances under the ‘Visual+SelfEnro’ setting.

All impairments negatively impact model performance. Among them, missing visuals have the most severe effect, while the other two types of impairments exhibit similar levels of degradation. However, the system with the contextual bank (System 4) maintains similar performance across different impairments and shows minimal degradation, indicating that contextual information can effectively compensate for degraded visuals.

In contrast, systems with speaker banks suffer significant degradation, especially when visuals are completely missing. However, they still outperform System 1. This suggests that

TABLE VIII: Comparison of SI-SNR and RTF for System 4 with contextual bank across different window length  $T_{win}$ .  $T_{init}$  and  $T_{sh}$  are set to 2s and 0.2s, respectively.

Sys. #	1s		1.5s		2s		3s		4s	
	SI-SNR (dB) ↑	RTF ↓	SI-SNR (dB) ↑	RTF ↓	SI-SNR (dB) ↑	RTF ↓	SI-SNR (dB) ↑	RTF ↓	SI-SNR (dB) ↑	RTF ↓
4	8.55	0.1082	9.86	0.1093	10.34	0.1103	10.40	0.1141	10.45	0.1422

TABLE IX: Comparison of SI-SNR and RTF for System 4 with contextual bank across different shift length  $T_{sh}$ .  $T_{init}$  and  $T_{win}$  are set to 2s and 2s, respectively.

Sys. #	0.05s		0.1s		0.2s		0.3s	
	SI-SNR (dB) ↑	RTF ↓	SI-SNR (dB) ↑	RTF ↓	SI-SNR (dB) ↑	RTF ↓	SI-SNR (dB) ↑	RTF ↓
4	8.84	0.5233	9.01	0.2341	10.34	0.1103	7.78	0.0733

these systems remain heavily reliant on visual cues, and adding additional speaker information is insufficient to maintain performance.

TABLE X: Comparison of whether using clean visual cues in the 0-th window step for self-enrollment speech (initialization step). These results are reported in SI-SNR (dB).

Visual Init	Sys. #				
	2	3	4	5	
Clean Visual	8.64	9.43	10.34	10.04	
Impaired Visual	7.33	8.53	8.91	9.11	

#### D. Impact of Visual Initialization

As shown in Table X, if we use impaired visual sequences as initialization in the 0-th window step, all systems' performance drops. This indicates that the quality of self-enrollment speech matters. If the self-enrollment contains errors, these errors could accumulate during the online processing. Therefore, it is better to use high-quality visual cues for initialization.

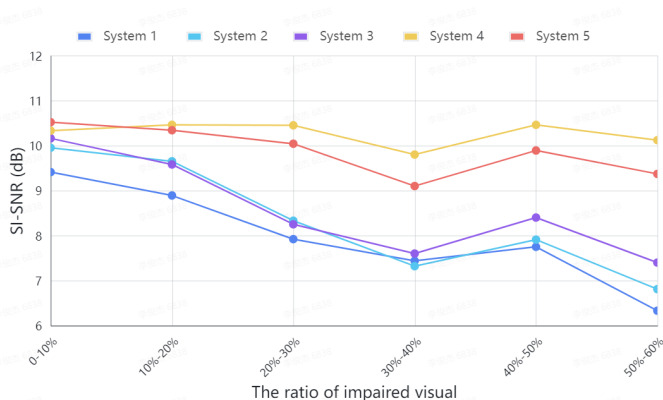


Fig. 8: The performance of different systems on different impaired ratios in online mode. Since in 0-th window step we set visual frames to clean, the impaired ratio of whole utterance is less higher than 60%.

#### E. Impact of Visual Impaired Ratio

Fig. 8 shows the performance across different impaired ratios of visual. We report System 1's performance under 'Visual Only' and other systems under 'Visual+SelfEnro'.

System 1 progressively deteriorates as the impairment ratio increases, which is expected. Systems 2 and 3 outperform the baseline model but still exhibit a similar trend. In contrast, Systems 4 and 5, which leverage contextual information, maintain nearly constant performance, showing minimal impact from impairments, as observed in Section V-C. This indicates that contextual information can effectively compensate for impaired visuals, providing a robust solution to visual impairments.

#### F. Ablation Studies

In this section, we examine the impact of various online parameters on both performance, measured by SI-SNR, and computational complexity, assessed via the real-time factor (RTF). The RTF is calculated on a single NVIDIA Tesla V100 GPU.

The online evaluation is conducted using a sliding window approach with a window length of  $T_{win}$ , shifting forward by  $T_{sh}$  at each step. The units of  $T_{win}$  and  $T_{sh}$  are in samples, but for convenience, we use seconds as the unit in this section.

In this section, we only report System 4's performance (contextual bank), cause it is our best system.

1) *Study on Window Length*: As shown in Table VIII, the RTF increases as the length of  $T_{win}$  increases because the models need to process a longer utterance for each sliding window. However, the performance in terms of SI-SNR increases due to model's extended receptive field.

2) *Study on Window Shifting Length*: As shown in Table IX, the RTF decreases as the length of  $T_{sh}$  increases, since a larger shift reduces the number of sliding windows required for online processing. The performance in terms of SI-SNR initially improves with increasing  $T_{sh}$ , but degrades when  $T_{sh}$  becomes too large. We hypothesize that a slightly larger shift  $T_{sh}$  improves perceptual consistency across sliding windows. This is likely because the normalization process in Equation 19 benefits from larger  $T_{sh}$  values. However, when  $T_{sh}$  becomes too large, the overlap between windows degrades, leading to a loss of contextual information continuity. This reduction in contextual information may negatively impact the model's ability to maintain attentional momentum, thus degrading performance.

3) *Study on Loss Function Weight*: As shown in Fig. 9, we compare the effect of different values of the weighting parameter  $\beta$  in Equation 17. The parameter  $\beta$  controls the

TABLE XI: Performance comparison between our proposed methods and other state-of-the-art (SOTA) models under impaired visual scenarios in the online mode. All MeMo systems are configured with the contextual bank only, and their performance is reported under the ‘Visual+SelfEnro’ setting. Star (\*) denotes models that are retrained on our impaired datasets for fair comparison.

Model	#Param (M)	Macs (G/s)	Impaired Visual			
			SI-SNR (dB) ↑	SDR (dB) ↑	PESQ ↑	STOI ↑
Mixture			0	0.09	1.26	0.63
ImagineNET [25]	33.61	518.95	8.97	9.40	1.92	0.82
MuSE [5], [20]	26.13	21.29	8.32	8.83	1.88	0.81
MoMuSE [20]	26.39	21.51	9.46	10.00	1.91	0.84
TDSE* [77]	22.15	20.03	8.13	8.53	1.85	0.81
MeMo (TDSE)	23.00	20.72	10.34	10.76	2.08	0.84
USEV* [6]	15.29	17.46	7.40	7.76	1.69	0.79
MeMo (USEV)	16.14	18.15	9.47	9.85	1.91	0.83
BSRNN* [79], [80]	31.17	224.06	7.98	8.07	1.83	0.78
MeMo (BSRNN)	32.23	224.93	10.98	9.47	2.01	0.83

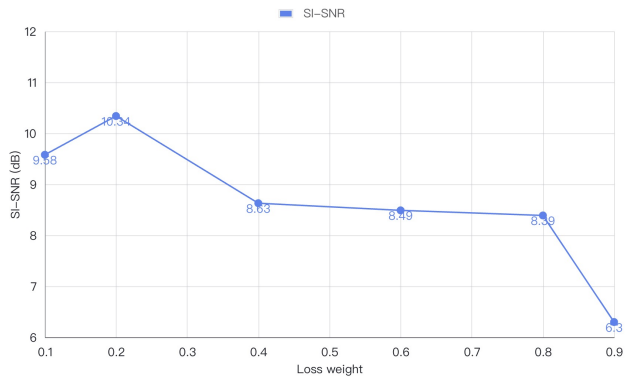


Fig. 9: Study for the effect of hyper-parameter  $\beta$  in the loss function.

trade-off between optimization in training Stage 1 and Stage 2. Since our final objective is to improve performance in Stage 2, a relatively small value of  $\beta$  is generally preferred. The results in the figure support this conclusion, with the best performance achieved when  $\beta = 0.2$ .

TABLE XII: Performance on the VoxCeleb-2mix-switch test set. In addition to utterance-level SI-SNR, we also report segmental SI-SNR, which evaluates performance over shorter speech segments to better reflect local variations in extraction quality. ‘Empty’ refers to the strategy of emptying the memory bank once a speaker switch point occurs within the model’s receptive field.

Sys.#	Segmental SI-SNR (dB)					SI-SNR (dB)
	0:2	2:4	4:8	8:12	12:16	
1	9.07	7.66	5.24	5.18	7.13	5.75
4	9.26	8.96	7.57	7.81	8.60	8.50
4+Empty	9.26	8.97	6.99	7.76	8.38	8.06

### G. Effectiveness on Switching Dataset

In this section, we investigate whether our proposed method can handle speaker-switching scenarios, as illustrated in

Fig. 7.<sup>10</sup> Results are reported in Table XII. Since MeMo with the contextual bank primarily relies on contextual information, we guess a target speaker switch during a conversation may disrupt the continuity of this context, potentially degrading performance. Hence, we also introduce a ‘Empty’ strategy that manually empties the contextual bank when a speaker switch point is detected within the model’s receptive field.

Overall, System 4 outperforms System 1 in both utterance-level SI-SNR and all segmental SI-SNR evaluations. During the 0–2s interval, only clean visual cues are used as reference; thus, both systems achieve similar performance. After 2s, when the visual cues become impaired, System 1 exhibits a notable performance drop, whereas System 4 degrades only slightly, demonstrating the robustness of leveraging contextual information. In the 4–8s segment, where the speaker switch occurs, both systems experience performance degradation. However, the decline is less pronounced for System 4, demonstrating its resilience under speaker-switching conditions. After the speaker switch, the performance of both systems begins to improve.

In addition, the ‘Empty’ strategy does not improve performance and even leads to a slight degradation. However, it still performs better than System 1, indicating that our proposed model inherently possesses the ability to handle speaker-switching scenarios with a degree of robustness. This suggests that the contextual bank can effectively adapt to dynamic changes in speaker identity over time. These findings further validate the resilience and adaptability of the proposed MeMo framework in challenging real-time conversational settings.

### H. Comparison with Other Models

In this section, we investigate the generalization ability of our proposed framework by applying the best-performing configuration, contextual bank, to various baseline models. As shown in Table XI, all models are evaluated under real-time settings. Firstly, models equipped with the contextual bank

<sup>10</sup>Note that all models are trained on the VoxCeleb-2mix dataset but evaluated on the VoxCeleb-2mix-switch dataset.

consistently outperform their counterparts across all evaluation metrics. Secondly, the contextual bank introduces only minimal additional parameters and negligible computational complexity. Finally, compared to prior studies, our proposed framework achieves superior performance on most evaluation metrics.

## VI. CONCLUSION

In this paper, we propose MeMo, a general and flexible framework designed to address the challenge of missing visual cues in real-time audio-visual target speaker extraction. MeMo incorporates two optional adaptive memory banks: the speaker bank and the contextual bank, which leverage historical information to maintain focus on the target speaker over time. While both banks contribute to performance improvements, the contextual bank demonstrates superior effectiveness. Experimental results validate the robustness of our proposed method across various challenging audio-visual scenarios.

## REFERENCES

- [1] E. C. Cherry, "Some experiments on the recognition of speech, with one and with two ears," *The Journal of the acoustical society of America*, vol. 25, no. 5, pp. 975–979, 1953.
- [2] A. W. Bronkhorst, "The cocktail party phenomenon: A review of research on speech intelligibility in multiple-talker conditions," *Acta acustica united with acustica*, vol. 86, no. 1, pp. 117–128, 2000.
- [3] J.-L. Schwartz, F. Berthommier, and C. Savariaux, "Seeing to hear better: evidence for early audio-visual interactions in speech identification," *Cognition*, vol. 93, no. 2, pp. B69–B78, 2004.
- [4] W. H. Sumby and I. Pollack, "Visual contribution to speech intelligibility in noise," *The journal of the acoustical society of america*, vol. 26, no. 2, pp. 212–215, 1954.
- [5] Z. Pan, R. Tao, C. Xu, and H. Li, "Muse: Multi-modal target speaker extraction with visual cues," in *ICASSP 2021 - 2021 IEEE International Conference on Acoustics, Speech and Signal Processing (ICASSP)*, 2021, pp. 6678–6682.
- [6] Z. Pan, M. Ge, and H. Li, "Useev: Universal speaker extraction with visual cue," *IEEE/ACM Trans. Audio, Speech and Lang. Proc.*, vol. 30, p. 3032–3045, sep 2022.
- [7] J. Wu, Y. Xu, S.-X. Zhang, L.-W. Chen, M. Yu, L. Xie, and D. Yu, "Time domain audio visual speech separation," in *2019 IEEE automatic speech recognition and understanding workshop (ASRU)*. IEEE, 2019, pp. 667–673.
- [8] K. Zmolikova, M. Delcroix, T. Ochiai, K. Kinoshita, J. Černocký, and D. Yu, "Neural target speech extraction: An overview," *IEEE Signal Processing Magazine*, vol. 40, no. 3, pp. 8–29, 2023.
- [9] D. Michelsanti, Z.-H. Tan, S.-X. Zhang, Y. Xu, M. Yu, D. Yu, and J. Jensen, "An overview of deep-learning-based audio-visual speech enhancement and separation," *IEEE/ACM Transactions on Audio, Speech, and Language Processing*, vol. 29, pp. 1368–1396, 2021.
- [10] Q. Liu, M. Ge, Z. Wu, and H. Li, "PIAVE: A Pose-Invariant Audio-Visual Speaker Extraction Network," in *Proc. INTERSPEECH 2023*, 2023, pp. 3719–3723.
- [11] Z. Pan, X. Qian, and H. Li, "Speaker extraction with co-speech gestures cue," *IEEE Signal Processing Letters*, vol. 29, pp. 1467–1471, 2022.
- [12] J. Li, M. Ge, Z. Pan, R. Cao, L. Wang, J. Dang, and S. Zhang, "Rethinking the Visual Cues in Audio-Visual Speaker Extraction," in *Proc. INTERSPEECH 2023*, 2023, pp. 3754–3758.
- [13] S.-W. Chung, S. Choe, J. S. Chung, and H.-G. Kang, "FaceFilter: Audio-Visual Speech Separation Using Still Images," in *Proc. Interspeech 2020*, 2020, pp. 3481–3485.
- [14] W. Wu, X. Chen, S. Wang, J. Wang, L. Meng, X. Wu, H. Meng, and H. Li, " $c^2$ av-tse: Context and confidence-aware audio visual target speaker extraction," *IEEE Journal of Selected Topics in Signal Processing* 2025.
- [15] W. Wu, S. Wang, X. Wu, H. Meng, and H. Li, "Incorporating linguistic constraints from external knowledge source for audio-visual target speech extraction," *Interspeech 2025*.
- [16] K. Li, R. Yang, F. Sun, and X. Hu, "Iianet: An intra- and inter-modality attention network for audio-visual speech separation," in *International Conference on Machine Learning*, 2024.
- [17] Y. Hu, R. Li, C. Chen, C. Qin, Q.-S. Zhu, and E. S. Chng, "Hearing lips in noise: Universal viseme-phoneme mapping and transfer for robust audio-visual speech recognition," in *Proceedings of the 61st Annual Meeting of the Association for Computational Linguistics*, 2023.
- [18] G. Sell, D. Snyder, A. McCree, D. Garcia-Romero, J. Villalba, M. Maciejewski, V. Manohar, N. Dehak, D. Povey, S. Watanabe *et al.*, "Diarization is hard: Some experiences and lessons learned for the jhu team in the inaugural dihard challenge," in *Interspeech*, 2018, pp. 2808–2812.
- [19] Y. Sun, H. Zhang, L. Wang, K. A. Lee, M. Liu, and J. Dang, "Noise-disentanglement metric learning for robust speaker verification," in *ICASSP 2023-2023 IEEE International Conference on Acoustics, Speech and Signal Processing (ICASSP)*. IEEE, 2023, pp. 1–5.
- [20] J. Li, K. Zhang, S. Wang, K. A. Lee, and H. Li, "Momuse: Momentum multi-modal target speaker extraction for real-time scenarios with impaired visual cues," *arXiv preprint arXiv:2412.08247*, 2024.
- [21] T. Pan, J. Liu, B. Wang, J. Tang, and G. Wu, "Ravss: Robust audio-visual speech separation in multi-speaker scenarios with missing visual cues," in *Proceedings of the 32nd ACM International Conference on Multimedia*, 2024, pp. 4748–4756.
- [22] M. Sadeghi and X. Alameda-Pineda, "Switching variational auto-encoders for noise-agnostic audio-visual speech enhancement," in *ICASSP 2021-2021 IEEE International Conference on Acoustics, Speech and Signal Processing (ICASSP)*.
- [23] X.-P. M. Sadeghi, "Robust unsupervised audio-visual speech enhancement using a mixture of variational autoencoders," in *ICASSP 2020-2020 IEEE International Conference on Acoustics, Speech and Signal Processing (ICASSP)*. IEEE, 2020, pp. 7534–7538.
- [24] Y. Wu, C. Li, J. Bai, Z. Wu, and Y. Qian, "Time-domain audio-visual speech separation on low quality videos," in *ICASSP 2022-2022 IEEE International Conference on Acoustics, Speech and Signal Processing (ICASSP)*. IEEE, 2022, pp. 256–260.
- [25] Z. Pan, W. Wang, M. Borsdorf, and H. Li, "Imaginet: Target speaker extraction with intermittent visual cue through embedding inpainting," in *ICASSP 2023 - 2023 IEEE International Conference on Acoustics, Speech and Signal Processing (ICASSP)*, 2023, pp. 1–5.
- [26] T. Afouras, J. S. Chung, and A. Zisserman, "My lips are concealed: Audio-visual speech enhancement through obstructions," in *Interspeech*, 2019.
- [27] J. Xu, J. Cui, Y. Hao, and B. Xu, "Multi-cue guided semi-supervised learning toward target speaker separation in real environments," *IEEE/ACM Transactions on Audio, Speech, and Language Processing*, 2023.
- [28] Y. Liu, Y. Deng, and Y. Wei, "A two-stage audio-visual speech separation method without visual signals for testing and tuples loss with dynamic margin," *IEEE Journal of Selected Topics in Signal Processing*, vol. 18, no. 3, pp. 459–472, 2024.
- [29] Y. Y. Liu and Y. Wei, "Cross-modal speech separation without visual information during testing," in *2023 IEEE Biomedical Circuits and Systems Conference (BioCAS)*. IEEE, 2023, pp. 1–5.
- [30] W. Ren, K.-H. Hung, R. Chao, Y. Li, H.-M. Wang, and Y. Tsao, "Robust audio-visual speech enhancement: Correcting misassignments in complex environments with advanced post-processing," in *2024 27th Conference of the Oriental COCODA International Committee for the Co-ordination and Standardisation of Speech Databases and Assessment Techniques*. IEEE, 2024, pp. 1–6.
- [31] D. S. Brungart and B. D. Simpson, "Cocktail party listening in a dynamic multitalker environment," *Perception & psychophysics*, vol. 69, no. 1, pp. 79–91, 2007.
- [32] G. Kidd, T. L. Arbogast, C. R. Mason, and F. J. Gallun, "The advantage of knowing where to listen," *The Journal of the Acoustical Society of America*, vol. 118, no. 6, pp. 3804–3815, 2005.
- [33] V. Best, E. J. Ozmeral, N. Kopčo, and B. G. Shinn-Cunningham, "Object continuity enhances selective auditory attention," *Proceedings of the National Academy of Sciences*, vol. 105, no. 35, pp. 13 174–13 178, 2008.
- [34] N. Ward, E. Paul, P. Watson, G. Cooke, C. Hillman, N. J. Cohen, A. F. Kramer, and A. K. Barbey, "Enhanced learning through multimodal training: evidence from a comprehensive cognitive, physical fitness, and neuroscience intervention," *Scientific reports*, vol. 7, no. 1, p. 5808, 2017.
- [35] J. G. Dingemans and A. Goedegebure, "The important role of contextual information in speech perception in cochlear implant users and its consequences in speech tests," *Trends in Hearing*.
- [36] B. Barton and A. A. Brewer, "Attention and working memory in human auditory cortex," in *The Human Auditory System*, S. Hatzopoulos, A. Ciorba, and P. H. Skarzynski, Eds. Rijeka: IntechOpen, 2019, ch. 1.

- [37] E. Awh, E. K. Vogel, and S.-H. Oh, "Interactions between attention and working memory," *Neuroscience*, vol. 139, no. 1, pp. 201–208, 2006.
- [38] B. Veluri, M. Itani, T. Chen, T. Yoshioka, and S. Gollakota, "Look once to hear: Target speech hearing with noisy examples," ser. CHI '24. New York, NY, USA: Association for Computing Machinery, 2024.
- [39] H. Sato, T. Ochiai, K. Kinoshita, M. Delcroix, T. Nakatani, and S. Araki, "Multimodal attention fusion for target speaker extraction," in *2021 IEEE Spoken Language Technology Workshop (SLT)*. IEEE, 2021, pp. 778–784.
- [40] T. Ochiai, M. Delcroix, K. Kinoshita, A. Ogawa, and T. Nakatani, "Multimodal speakerbeam: Single channel target speech extraction with audio-visual speaker clues," in *INTERSPEECH*, 2019, pp. 2718–2722.
- [41] J. Weston, S. Chopra, and A. Bordes, "Memory networks," *International Conference on Learning Representations, ICLR 2015*.
- [42] S. Sukhbaatar, J. Weston, R. Fergus *et al.*, "End-to-end memory networks," *Advances in neural information processing systems*, vol. 28, 2015.
- [43] Z. Wu, Y. Xiong, S. X. Yu, and D. Lin, "Unsupervised feature learning via non-parametric instance discrimination," in *Proceedings of the IEEE conference on computer vision and pattern recognition*, 2018, pp. 3733–3742.
- [44] M. Kim, J. Hong, S. J. Park, and Y. M. Ro, "Cromm-vs-r: Cross-modal memory augmented visual speech recognition," *IEEE Transactions on Multimedia*, vol. 24, pp. 4342–4355, 2022.
- [45] J. H. Yeo, M. Kim, and Y. M. Ro, "Multi-temporal lip-audio memory for visual speech recognition," in *ICASSP 2023 - 2023 IEEE International Conference on Acoustics, Speech and Signal Processing (ICASSP)*, 2023, pp. 1–5.
- [46] M. Kim, J. Hong, S. J. Park, and Y. M. Ro, "Multi-modality associative bridging through memory: Speech sound recollected from face video," *2021 IEEE/CVF International Conference on Computer Vision (ICCV)*, pp. 296–306, 2021.
- [47] J. H. Yeo, M. Kim, J. Choi, D. H. Kim, and Y. M. Ro, "Akvsr: Audio knowledge empowered visual speech recognition by compressing audio knowledge of a pretrained model," *IEEE Transactions on Multimedia*, 2024.
- [48] M. Kim, J. H. Yeo, and Y. M. Ro, "Distinguishing homophones using multi-head visual-audio memory for lip reading," in *AAAI Conference on Artificial Intelligence*, 2022.
- [49] J. Hong, M. Kim, S. J. Park, and Y. M. Ro, "Speech reconstruction with reminiscence sound via visual voice memory," *IEEE/ACM Transactions on Audio, Speech, and Language Processing*, vol. 29, pp. 3654–3667, 2021.
- [50] J. Xu, J. Shi, G. Liu, X. Chen, and B. Xu, "Modeling attention and memory for auditory selection in a cocktail party environment," in *AAAI Conference on Artificial Intelligence*, 2018.
- [51] A. Bellur, K. Thakkar, and M. Elhilali, "Explicit-memory multiresolution adaptive framework for speech and music separation," *Eurasip Journal on Audio, Speech, and Music Processing*, vol. 2023, 2023.
- [52] J. Li, K. Zhang, S. Wang, H. Li, M.-W. Mak, and K. A. Lee, "On the effectiveness of enrollment speech augmentation for target speaker extraction," in *2024 IEEE Spoken Language Technology Workshop (SLT)*. IEEE, 2024, pp. 325–332.
- [53] Z. Pan, R. Tao, C. Xu, and H. Li, "Selective listening by synchronizing speech with lips," *IEEE/ACM Transactions on Audio, Speech, and Language Processing*, vol. 30, pp. 1650–1664, 2022.
- [54] C. Deng, S. Ma, Y. Sha, Y. Zhang, H. Zhang, H. Song, and F. Wang, "Robust Speaker Extraction Network Based on Iterative Refined Adaptation," in *Proc. Interspeech 2021*.
- [55] Z.-X. Li, Y. Song, L.-R. Dai, and I. McLoughlin, "Listening and grouping: an online autoregressive approach for monaural speech separation," *IEEE/ACM Transactions on Audio, Speech, and Language Processing*, vol. 27, no. 4, pp. 692–703, 2019.
- [56] Z.-X. Li, Y. Song, L.-R. Dai, and I. McLoughlin, "Source-aware context network for single-channel multi-speaker speech separation," in *2018 IEEE ICASSP*.
- [57] H. Wang, Y. Song, Z.-X. Li, I. McLoughlin, and L.-R. Dai, "An online speaker-aware speech separation approach based on time-domain representation," in *ICASSP 2020-2020 IEEE International Conference on Acoustics, Speech and Signal Processing (ICASSP)*. IEEE, 2020, pp. 6379–6383.
- [58] P. Andreev, N. Babaev, A. Saginbaev, I. Shchekotov, and A. Alanov, "Iterative autoregression: a novel trick to improve your low-latency speech enhancement model," in *INTERSPEECH 2023*, 2023.
- [59] Z. Pan, M. Borsdorf, S. Cai, T. Schultz, and H. Li, "Neuroheed: Neuro-steered speaker extraction using eeg signals," *IEEE/ACM Transactions on Audio, Speech, and Language Processing*, 2024.
- [60] Z. Pan, G. Wichern, F. G. Germain, S. Khurana, and J. Le Roux, "Neuroheed+: Improving neuro-steered speaker extraction with joint auditory attention detection," in *2024 IEEE ICASSP*.
- [61] Z. Pan, G. Wichern, F. G. Germain, K. Saijo, and J. Le Roux, "Paris: Pseudo-autoregressive siamese training for online speech separation," in *Interspeech 2024*.
- [62] Z. Pan, W. Wang, S. Zhao, C. Zhang, K. Zhou, Y. Ma, and B. Ma, "Online audio-visual autoregressive speaker extraction," *arXiv preprint arXiv:2506.01270*, 2025.
- [63] A. Vaswani, N. Shazeer, N. Parmar, J. Uszkoreit, L. Jones, A. N. Gomez, L. Kaiser, and I. Polosukhin, "Attention is all you need," *Advances in neural information processing systems*, vol. 30, 2017.
- [64] B. Desplanques, J. Thienpondt, and K. Demuynck, "Ecapa-tdnn: Emphasized channel attention, propagation and aggregation in tdnn based speaker verification," in *Interspeech 2020*, 2020, pp. 3830–3834.
- [65] H. Wang, C. Liang, S. Wang, Z. Chen, B. Zhang, X. Xiang, Y. Deng, and Y. Qian, "Wespeaker: A research and production oriented speaker embedding learning toolkit," in *ICASSP 2023-2023 IEEE International Conference on Acoustics, Speech and Signal Processing (ICASSP)*.
- [66] Y. Bengio, J. Louradour, R. Collobert, and J. Weston, "Curriculum learning," in *Proceedings of the 26th annual international conference on machine learning*, 2009, pp. 41–48.
- [67] R. J. Williams and D. Zipser, "A learning algorithm for continually running fully recurrent neural networks," *Neural computation*, vol. 1, no. 2, pp. 270–280, 1989.
- [68] S. Bengio, O. Vinyals, N. Jaitly, and N. Shazeer, "Scheduled sampling for sequence prediction with recurrent neural networks," *Advances in neural information processing systems*, vol. 28, 2015.
- [69] K. T. R. Voo, L. Jiang, and C. C. Loy, "Delving into high-quality synthetic face occlusion segmentation datasets," *2022 IEEE/CVF Conference on Computer Vision and Pattern Recognition Workshops (CVPRW)*, pp. 4710–4719, 2022.
- [70] J. Hong, M. Kim, J. Y. Choi, and Y. M. Ro, "Watch or listen: Robust audio-visual speech recognition with visual corruption modeling and reliability scoring," *2023 IEEE/CVF Conference on Computer Vision and Pattern Recognition (CVPR)*, 2023.
- [71] J. S. Chung, A. Nagrani, and A. Zisserman, "Voxceleb2: Deep speaker recognition," in *INTERSPEECH*, 2018.
- [72] W. Wu, X. Chen, X. Wu, H. Li, and H. Meng, "Avhumar: Audio-visual target speech extraction with pre-trained av-hubert and mask-and-recover strategy," *CVPR 2024 Sight and Sound Workshop*, 2024.
- [73] W. Wu, X. Chen, X. Wu, H. Li, and H. Meng, "Target speech extraction with pre-trained av-hubert and mask-and-recover strategy," in *2024 International Joint Conference on Neural Networks (IJCNN)*, 2024.
- [74] J. Le Roux, S. Wisdom, H. Erdogan, and J. R. Hershey, "Sdr-half-baked or well done?" in *2019 IEEE ICASSP*.
- [75] A. W. Rix, J. G. Beerends, M. P. Hollier, and A. P. Hekstra, "Perceptual evaluation of speech quality (pesq)-a new method for speech quality assessment of telephone networks and codecs," in *2001 IEEE ICASSP*.
- [76] C. H. Taal, R. C. Hendriks, R. Heusdens, and J. Jensen, "A short-time objective intelligibility measure for time-frequency weighted noisy speech," in *2010 IEEE ICASSP*.
- [77] J. Wu, Y. Xu, S.-X. Zhang, L.-W. Chen, M. Yu, L. Xie, and D. Yu, "Time domain audio visual speech separation," in *2019 IEEE Automatic Speech Recognition and Understanding Workshop (ASRU)*, 2019, pp. 667–673.
- [78] Y. Luo and N. Mesgarani, "Conv-tasnet: Surpassing ideal time-frequency magnitude masking for speech separation," *IEEE/ACM Transactions on Audio, Speech, and Language Processing*, vol. 27, no. 8, pp. 1256–1266, 2019.
- [79] Y. Luo and J. Yu, "Music source separation with band-split rnn," *IEEE/ACM Transactions on Audio, Speech, and Language Processing*, vol. 31, pp. 1893–1901, 2023.
- [80] S. Wang, K. Zhang, S. Lin, J. Li, X. Wang, M. Ge, J. Yu, Y. Qian, and H. Li, "Wesep: A scalable and flexible toolkit towards generalizable target speaker extraction," in *Proc. Interspeech 2024*, 2024, pp. 4273–4277.